Tu N104 13

Marine Survey Design and Analysis Using All Multiples

A. Kumar* (Delft University of Technology), G. Blacquiere (Delft University of Technology), M. W. Pedersen (PGS Geophysical AS) & A. Goertz (PGS Geophysical AS)

SUMMARY

Despite a tremendous leap in efficiency and wave field sampling over the last two decades, it is sometimes still difficult to achieve adequate coverage and resolution with marine streamer acquisition. It is therefore necessary to carefully study the acquisition geometry, especially with respect to resolution and image quality in the cross-line direction. In this paper, we extend the focal beam method to analyze marine streamer geometries with and without using all multiples. Multiples are traditionally suppressed, but can instead be used in the imaging process where they often contribute positively by opening up the available aperture. We especially address coverage deficiencies that can occur when the survey geometry deviates from the ideal, for example due to feathering. As a result, extra 'infill' lines must be acquired. We present how infill analysis can be performed via the focal beam theory to assess the impact of coverage holes for primaries as well as multiples.

Introduction

Marine streamer acquisition has improved significantly during the last decade, extending from conventional 3-D marine towed streamer seismic acquisition to the more recent developments such as wide-azimuth, full-azimuth towed streamer, broadband techniques, coil shooting and the emerging technology of simultaneous source, or blended, acquisition. Recent developments have been focusing on improving the sampling of the wavefield especially in the cross-line direction to enhance the resolution and image quality. In this paper, we extend our existing acquisition analysis technology, the so-called focal beam method further to analyze marine streamer geometries. Furthermore, utilization of multiples in imaging is an emerging methodology, and therefore, we also include multiples as a signal in our acquisition analysis and show that multiples provide additional angles.

During marine streamer acquisition, coverage deficiencies can occur when the vessel or sail-line geometry deviates from the ideal, for example due to feathering. As a result, extra 'infill' lines must be acquired. Day and Rekdal (2006) developed geophysical-based infill specifications to assess the impact of coverage holes on data quality, and thereby set suitable specifications based on permitted levels of data degradation. We performed similar infill analysis via the focal beam theory to assess the impact of coverage holes for the primaries as well as the multiples. The infill estimation by Day and Rekdal (2006) was based on time migrated images, by doing this analysis via focal beams, we extend this work to depth-migrated images with or without using multiples.

Focal beam analysis extended to multiples

Focal beam analysis makes use of the so-called common focus point (CFP) technology (Berkhout, 1997) in which a seismic response can be composed from grid-point responses, and the migration result can be simulated for a specific grid-point by the double focusing concept. In the focal beam method, the aim is to find the angle-dependent effects introduced by the acquisition geometry, irrespective of any angle-dependent subsurface properties at the target level (van Veldhuizen et al., 2008). Therefore, grid-point responses in the modeling are chosen to be angle-independent, i.e., responses due to unit point diffractors. Using the matrix operator notation, the monochromatic seismic response for an angle-independent grid-point response for the n^{th} stationary part of the total survey can be written as:

$$\delta_k \mathbf{P}^{[n]}(z_0;z_0) = \mathbf{D}^{[n]}(z_0)\mathbf{W}^{-}(z_0,z_m)\delta_k \mathbf{R}^{\cup}(z_m,z_m)\mathbf{W}^{+}(z_m,z_0)\mathbf{S}^{[n]}(z_0). \tag{1}$$

In this equation, $\mathbf{W}^{+}(z_m,z_0)$ and $\mathbf{W}^{-}(z_0,z_m)$ are one-way propagation matrices, which describe respectively the down and upward wave propagation through a heterogeneous layer between depth levels z_0 and z_m. $\delta_k \mathbf{R}^{\cup}(z_m,z_m)$ represents angle-independent grid-point reflectivity at depth level z_m. The superscript '$\cup$' indicates that the reflection turns a downward traveling wavefield into an upward traveling wavefield. The matrices **D** and **S** describe detector and source properties, respectively. The double focusing result of equation (1) can be written as:

$$\begin{aligned} \delta_k \mathbf{P}^{[n]}(z_m;z_m) &= \mathbf{F}(z_m,z_0)\delta_k \mathbf{P}^{[n]}(z_0;z_0)\mathbf{F}(z_0,z_m), \\ &= \mathbf{F}(z_m,z_0)\mathbf{D}^{[n]}(z_0)\mathbf{W}^{-}(z_0,z_m)\delta_k \mathbf{R}^{\cup}(z_m,z_m)\mathbf{W}^{+}(z_m,z_0)\mathbf{S}^{[n]}(z_0)\mathbf{F}(z_0,z_m). \end{aligned} \tag{2}$$

where matrix **F** represents the focusing operator which removes the effects of one way propagation of $\mathbf{W}^{+}$ and $\mathbf{W}^{-}$. Basically, by doing the double focusing, the data matrix $\delta_k \mathbf{P}^{[n]}(z_0;z_0)$ is downward extrapolated to the depth level of the involved grid-point, resulting in the so-called grid-point matrix $\delta_k \mathbf{P}^{[n]}(z_m;z_m)$. Considering $\delta_k \mathbf{R}^{\cup}(z_m,z_m)$ is a unit angle-independent matrix, the double focusing results (equation 2) can be further reduced to the following expression:

$$\begin{aligned} \delta_k \mathbf{P}^{[n]}(z_m;z_m) &= \left[\mathbf{F}(z_m,z_0)\mathbf{D}^{[n]}(z_0)\vec{W}_k(z_0,z_m)\right]\left[\vec{W}_k^{\dagger}(z_m,z_0)\mathbf{S}^{[n]}(z_0)\mathbf{F}(z_0,z_m)\right], \\ &= \vec{D}_k^{[n]}(z_m,z_m)\vec{S}_k^{\dagger[n]}(z_m,z_m). \end{aligned} \tag{3}$$

where $\vec{D}_k^{[n]}(z_m,z_m)$ and $\vec{S}_k^{\dagger[n]}(z_m,z_m)$ represent the focal detector beam (a column vector) and the focal source beam (a row vector) for the k^{th} grid-point by the n^{th} stationary part of the total survey, respectively.

A row vector is marked by a dagger symbol (†). Note that, the superscripts '+' and '−' from the wave propagation term **W** have been removed now, for simplicity.

If we include multiples at the source side, the one-way downward propagator $\mathbf{W}^{+}(z_m, z_0)$ in equation (1) is replaced by the full-wavefield propagator $\mathbf{G}^{+}(z_m, z_0)$, which includes the effects of all multiples (i.e., propagation as well as reflection and transmission effects). Similarly, if we include multiples at the detector side, one-way upward propagator $\mathbf{W}^{-}(z_0, z_m)$ in equation (1) is replaced by the full-wavefield propagator $\mathbf{G}^{-}(z_0, z_m)$.

In the present focal beam analysis method, the two focal beams are computed separately and analyzed in the spatial as well as in the Radon domain. They are usually combined in the Radon domain by assuming a unit horizontal reflector at the target point to provide an AVP (amplitude versus ray parameter) function. Optimally the AVP function should be unity within the available wavenumber band. However, the AVP function for the streamer geometries yields a very limited range of angles, which in turn makes it difficult to assess such geometries. If we combine these two beams by assuming a point diffractor at the target point instead of a reflector, we analyze the geometry performance for diffractions. We elaborate the discussion further on the grid-point matrix (equation 3) and subsequently derive the weighted focal beams concept for the assessment of marine streamer geometries for diffractions.

According to equation (3), the grid-point matrix $\delta_k \mathbf{P}^{[n]}(z_m; z_m)$ can be obtained by the matrix multiplication of the focal detector beam and the focal source beam. In this matrix, the diagonal elements represent the seismic image of the k^{th} grid-point at depth level z_m, the so-called resolution function. However, the elements in the k^{th} column of this matrix represent the weighted focal detector beam, where the weighting is related to the k^{th} element of the focal source beam. Similarly, the elements in the k^{th} row of this matrix represent the weighted focal source beam, where the weighting is related to the k^{th} element of the focal detector beam. This is shown in Figure 1.

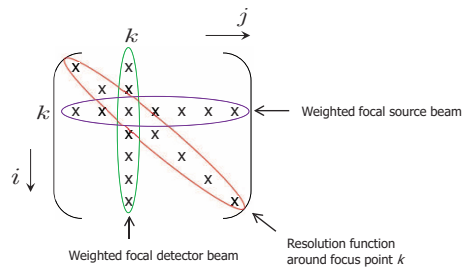

Figure 1 *The schematic representation of grid-point matrix. The letters i and j indicate the location number varying laterally.*

To get a quantitative impression of the total illumination and sensing for all sources and detectors included in the survey, the weighted focal beams for each template should be summed.

EXAMPLES

To illustrate the concept of weighted focal beams, we performed focal beam analysis to marine streamer geometries for primaries as well as multiples. In the case of marine streamer geometries, the location of the detectors moves with the source position. Therefore, the focal beams are computed per stationary geometry, i.e., for each shot position. The sum of the weighted focal beams for the total survey is shown in the following.

The acquisition geometry comprises a single source and 12 streamers. The in-line source separation is 50 m and the streamer separation is 100 m. The in-line hydrophone spacing is 25 m and the length of the streamer is 1200 m. The nearest offset is 50 m. There are 4 sail lines having 600 m sail-line separation. The subsurface is a simple 3-D plane layer model where the velocity increases with depth. The middle cross-section of the model is shown in Figure 2a. The analysis is carried out for the range of frequencies from 2 to 30 Hz. A target point laterally located at the center of the total survey area has been chosen for the analysis (indicated by the red star in the Figure 2a). The target depth is defined at 700 m. Note that only 4 sail-lines are considered here, as additional sail-lines would not contribute much to the imaging of the considered target point.

The sum of the weighted focal beams in the spatial domain for the total survey is shown in Figures

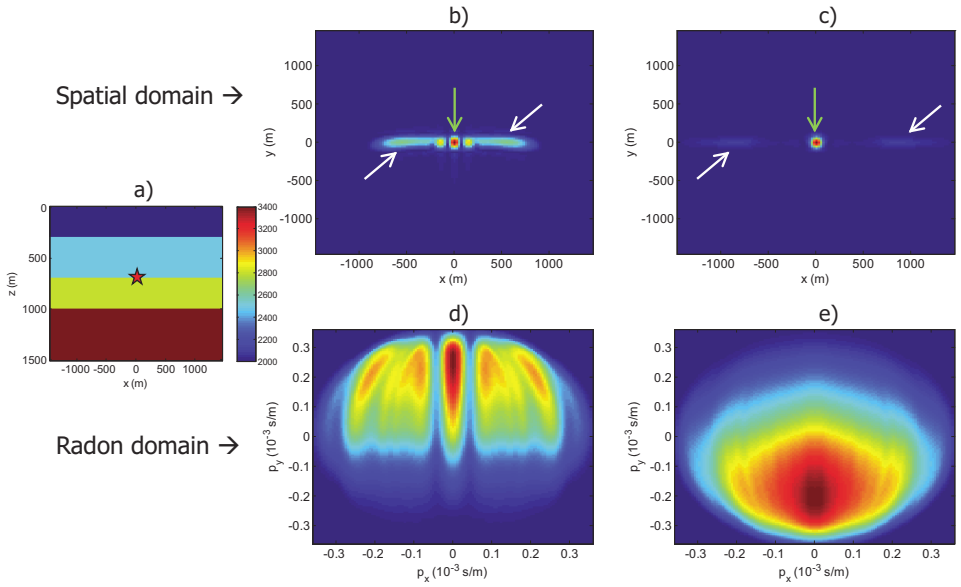

Figure 2 *a) 2-D cross section of 3-D plane layer subsurface model, b) the sum of weighted focal source beams for the total survey in the spatial domain, c) the sum of weighted focal detector beams in the spatial domain, d) the sum of weighted focal source beams in the Radon domain, e) the sum of weighted focal detector beams in the Radon domain. The white arrows indicate the side lobes while the green arrows point towards the main lobe.*

2b and c. The results are displayed in a linear amplitude scale. The large spacing between the source lines and the detector lines results in spatial aliasing effects. Spatial aliasing causes the side lobes in the cross-line directions that are visible in Figures 2b and c. The side-lobe level for the detector beam is much lower than that of the source beam. This can be explained by the much denser sampling in the cross-line direction for the detectors. Comparison of the side-lobe position shows that for a smaller line spacing, the side lobes are farther away from the main lobe and also weaker in amplitude.

The angle-dependent information contained in these beams can be obtained by the Radon transformation. Figure 2d shows illumination angles weighted by the strength of the focused detectors. Similarly, Figure 2e provides sensing angles weighted by the strength of the focused sources. Again, due to large source-line spacing in the example, we see spatial aliasing effects in this domain as a strong amplitude in the middle of Figure 2d. The detector geometry imprint can be seen as stripes in Figure 2e, which suggest that a denser detector sampling is needed in the cross-line direction.

So far, we have seen the results of the focal beam analysis for the primaries-only wavefield. Now, we provide the results for the case that multiples are included. In the example discussed above, we include multiples at the detector side. Therefore, the focal detector beam needs to be recomputed. Figure 3 shows the comparison of the sum of the weighted focal detector beams for the primaries-only wavefield versus the full wavefield. In this simple layer-model case, multiples provide additional small angles which increase the amplitude around these small angles and in turn mask the detector imprint in the narrow angle range.

Next, we analyze the effects of coverage holes on the sum of the weighted focal detector beams for the same model. Coverage holes in CMP positions are simulated by removing more and more streamers from two adjacent central sail-lines. Figure 4 shows the result of this analysis for the primaries as well as for the full wavefield. In the upper row of Figure 4, it is clear that with increase in hole size, gaps around the zero degree angle range increase and the amplitudes of these angles decrease. However, multiples succeed to boost these amplitude as well as to fill in the smaller angles to some extent, as is clear from

the lower row of Figure 4. With this analysis, we can define criteria for the acceptable gap size in the seismic data similar to the criterion discussed in Day and Rekdal (2006).

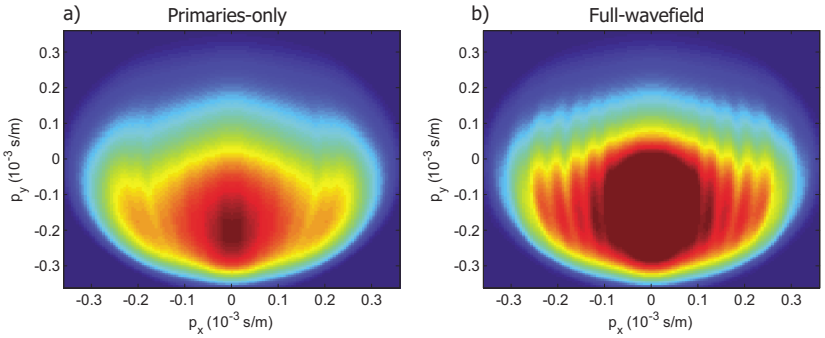

Figure 3 *Comparison of a) the sum of the weighted focal detector beams for primaries-only wavefield versus b) for the full wavefield.*

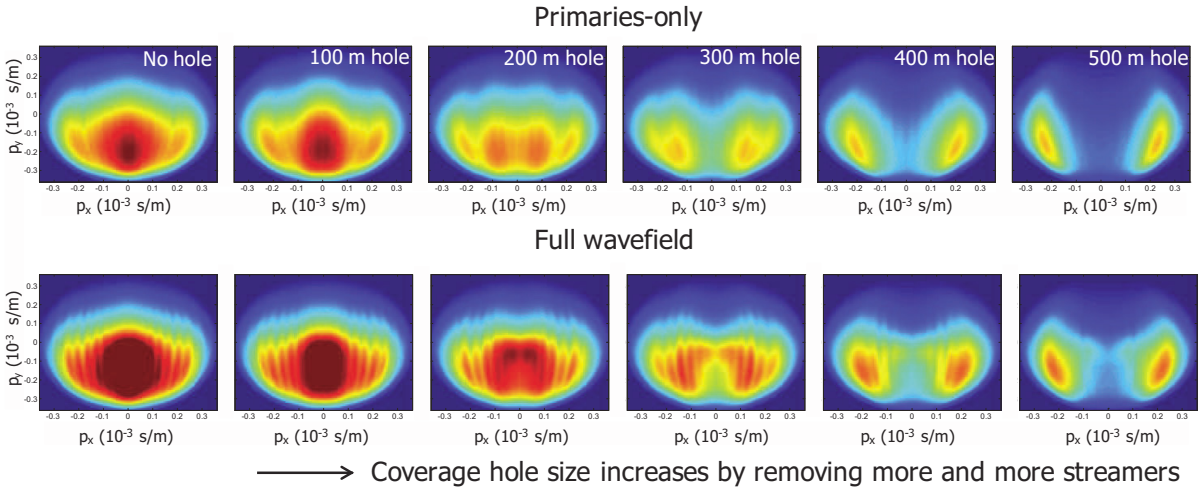

Figure 4 *The upper row shows the variations in sum of the weighted focal detector beams with hole size increment for primaries-only wavefield. The lower row shows the same for the full wavefield.*

Conclusions

The concept of weighted focal beams for diffraction analysis is introduced and demonstrated via a scaled 3-D marine streamer acquisition example. It is shown that multiples help in suppressing the acquisition geometry imprint in the narrow angle range for the simple layer model case. This supports the theory that multiples imaging uses an areal, down-going illuminating wavefield, which is broadly distributed everywhere in the subsurface compared to the point source illumination in the case of primaries-only imaging. Furthermore, this concept can be used to assess the impact of coverage holes on data quality and to predict the infill requirements with or without using multiples.

Acknowledgments

The authors thank PGS Geophysical AS for their support and consent for publication of this paper.

References

Berkhout, A.J. [1997] Pushing the limits of seismic imaging, part I: prestack migration in terms of double dynamic focusing. GEOPHYSICS, **62**(3), 937–953.

Day, A. and Rekdal, T. [2006] Determining infill specifications based on geophysical criteria. *76th Annual International Meeting, SEG, Expanded Abstracts*, 30–35.

van Veldhuizen, E.J., Blacquière, G. and Berkhout, A.J. [2008] Acquisition geometry analysis in complex 3D media. GEOPHYSICS, **73**(5), Q43–Q58.